

Cruising Performance of a Large Passenger Ship in Heavy Sea

Toshifumi Fujiwara and Michio Ueno
National Maritime Research Institute
Tokyo, Japan

Yoshiho Ikeda
Department of Marine System Engineering
University of Osaka Prefecture
Osaka, Japan

ABSTRACT

The authors proposed a new estimation method of wind forces and moments acting on ships based on a physical-component-model of the wind loads. In this paper, using the wind loads estimation method, steady cruising performances of a large passenger ship are estimated in heavy sea in order to assess the strong wind and waves effects. Some important characteristics of the resistance increase in steady cruising condition in heavy sea for the large passenger ship are clearly revealed in the calculation.

KEY WORDS: Cruising performance, Large passenger ship, Heavy sea, Wind and waves, Wind loads estimation, Resistance increase, MMG model.

INTRODUCTION

The accurate estimation of wind and waves effects for a ship is very important for assessing its operational cost. Especially a large passenger ship with large superstructures is significantly affected by strong wind. The authors proposed a new estimation method of wind forces and moments acting on ships based on a physical-component-model of the wind loads, consisting of the longitudinal-flow drag, cross-flow drag, lift and induced drag (Fujiwara et al, 2006a). In this paper, using the new wind loads estimation method, steady cruising performances of a large passenger ship are calculated under strong wind and waves from the view points of the assessment of the wind effect.

Naito et al. (1998) evaluated the steady performances of VLCC with the effect of drift, rudder forces under wind and waves. Yuasa et al. (1986) measured the real PCC ship performance using a monitoring system for ship speed, hull stress etc. for 2 years. Large passenger ship, however, have never been treated to assess the ship performance in the sea for the economical and safety aspects. The authors (Fujiwara et al., 2006b) assessed the steady cruising performance of a large passenger ship under strong wind. The results showed the some important characteristics on the ship with large superstructures. Strong wind

brought the large passenger ship to large drift, heel and rudder angles. In this paper, the assessment of the ship performances in heavy sea is conducted.

The steady-state equations are formulated based on the MMG model (Hirano et al., 1982, Kijima et al., 1990, Fujiwara et al., 2005) for ship manoeuvring simulation to obtain the steady ship conditions like the ship speed, drift, heel and rudder angles. The hydrodynamic hull forces are decided by the experimental results in a towing tank. The rudder forces and rudder-hull interaction effects are obtained from latest estimation methods (Kijima et al., 1990, 1999, Fujii et al., 1961). The wind loads used in the calculation includes the effect of boundary layer profile of wind and ship inclination (Fujiwara et al., 2006b). Steady wave loads are also estimated using the proposed method by the one of the authors (Ueno et al., 2000), Maruo(1957) and Fujii et al.(1967).

As a result, the resistance increase in steady cruising conditions in heavy wind and waves for the large passenger ship are clearly understood. The wind of closed hauled and broad reach, that is front and back side oblique wind, has very important role for resistance increase of the ship rather than head wind. Although one usually thinks the wave forces are dominant for the resistance increase of a ship, in case of the large passenger ship, strong wind gives large effect on the resistance increase rather than waves. Moreover, change of DHP (Delivered House Power) of the ship in wind and waves is clarified.

FORMULATION OF STEADY-STATE EQUATIONS IN THE SEA

In this section, the governing equations and the steady-state conditions are presented with the calculation method of hydrodynamic and aerodynamics loads. The governing equations of motion are modeled using the MMG formulation (Hirano et al., 1982, Kijima et al., 1990).

Ship motion equations

The coordination is represented as Fig. 1. Steady navigating will persist when there are no rates of change of the ship motion parameters the longitudinal, lateral and yaw velocities with respect to the center of

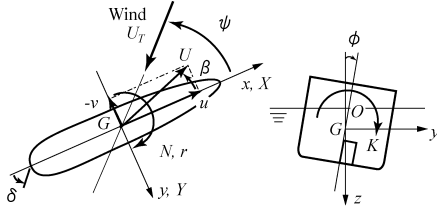


Fig. 1 Coordinate systems and definitions of force and moment sign convention for ship hull loading

gravity of the ship u, v, \dot{r} and heel angle ϕ . The conditions of steady cruising reduce the terms to the four following mathematical equations:

$$\begin{aligned} X &= 0, \quad Y = 0, \quad N = 0 \\ K - W \cdot \overline{GM} \sin \phi &= 0 \end{aligned} \quad (1)$$

Here, X, Y, N and K are the longitudinal, lateral external forces and yaw, heel moments defined in Fig. 1. W, \overline{GM} are the displacement of a ship and the transverse metacentric height. These equations will be solved for the steady advance speed of the ship, drift, heel and rudder angles, U, β, ϕ & δ respectively, for different true wind speeds, U_T , and direction, ψ (Fujiwara et al., 2006b).

External loads experienced by ship

Using the suffices H, P, R, A and W to indicate the contribution of the hull, propeller, rudder, wind and waves to the external forces and moments one may write:

$$\begin{aligned} X &= X_{H0} + X_H + X_P + X_R + X_A + X_W \\ Y &= Y_H + Y_R + Y_A + Y_W \\ N &= N_H + N_R + N_A + N_W \\ K &= K_H + K_R + K_A \end{aligned} \quad (2)$$

The definitions of each term are presented in following sections.

Hull Hydrodynamic Loads

The calm water resistance X_{H0} and the hydrodynamic hull forces X_H depended on the drift and heel angles in Eq. 2 are provided from towing tank model tests undertaken in the University of Osaka Prefecture (Tank size; 70m by 3m by 1.6m). Measured values of X_{H0} are captured in the polynomial expression using Froude number F_R in $0.10 \leq F_R \leq 0.32$:

$$\begin{aligned} X'_{H0} &= X_{H0} / \frac{\rho}{2} L_{PP} d U^2 \\ &= R_0 + R_1 F_R + R_2 F_R^2 + R_3 F_R^3 + R_4 F_R^4 \end{aligned} \quad (3)$$

The superscripted prime of X_{H0} indicates non-dimensional quantity using the water density ρ , the length between perpendiculars L_{PP} and the draft d . In $F_R \leq 0.10$, when the ship has slow forward speed, the extrapolated straight line continuing from Eq. (3) is used in the calculation.

To take into account the influences of the drift and heel angles the resulting forces and moments acting on the underwater hull are expressed in the following hydrodynamic derivative forms:

$$\begin{aligned} X'_H &= X_H / \frac{\rho}{2} L_{PP} d U^2 \\ &= X'_{H0} + X'_{\beta\beta} \beta^2 + X'_{\beta\phi} \beta \phi + X'_{\phi\phi} \phi^2 + X'_{\beta\beta\beta} \beta^3 \\ Y'_H &= Y_H / \frac{\rho}{2} L_{PP} d U^2 \\ &= Y'_{\beta} \beta + Y'_{\phi} \phi + Y'_{\beta\beta\beta} \beta^3 + Y'_{\beta\beta\phi} \beta^2 \phi + Y'_{\beta\phi\phi} \beta \phi^2 + Y'_{\phi\phi\phi} \phi^3 \\ N'_H &= N_H / \frac{\rho}{2} L_{PP}^2 d U^2 \\ &= N'_{\beta} \beta + N'_{\phi} \phi + N'_{\beta\beta\beta} \beta^3 + N'_{\beta\beta\phi} \beta^2 \phi + N'_{\beta\phi\phi} \beta \phi^2 + N'_{\phi\phi\phi} \phi^3 \\ K'_H &= K_H / \frac{\rho}{2} L_{PP} d^2 U^2 \\ &= K'_{\beta} \beta + K'_{\phi} \phi + K'_{\beta\beta\beta} \beta^3 + K'_{\beta\beta\phi} \beta^2 \phi + K'_{\beta\phi\phi} \beta \phi^2 + K'_{\phi\phi\phi} \phi^3 \end{aligned} \quad (4)$$

Propeller and rudder Loads

The propeller thrust force X_P is determined in a manner consistent with the MMG model (Kijima et al., 1990) using:

$$X_P = (1 - t_p) n^2 D_p^4 K_T(J) \quad (5)$$

That is, the propeller thrust is dependent upon the thrust deduction factor, t_p , the rotational velocity of the propeller, n , the propeller diameter, D_p and the thrust coefficient with the advance coefficient, $K_T(J)$. The advance coefficient J including wake fraction are also defined in accordance with the MMG model.

The rudder forces and moments are defined in terms of the Kijima et al. (1990) coefficients a_H, x'_H and t_R , the rudder orientation, δ , and the associated resultant normal rudder force, F_N . The rudder loads are defined as follows:

$$\begin{aligned} X_R &= -(1 - t_R) F_N \sin \delta \\ Y_R &= -(1 + a_H) F_N \cos \delta \\ N_R &= -(x'_R + a_H x'_H) (1 + l_{CB} / L_{PP}) F_N \cos \delta \\ K_R &= (1 + a_H) z'_R F_N \cos \delta \end{aligned} \quad (6)$$

The non-dimensional coordinates $x'_R = x_R / L_{PP}$ and $z'_R = z_R / d$ are associated with the rudder point defined as the intersection of the vertical line through the aft perpendicular and the horizontal center line of the rudder below the undisturbed free surface. The position of this selected point is defined with respect to the origin located at the intersection of the still water plane, the amidships section and the longitudinal plane of ship symmetry.

The coefficient values for $a_H, x'_H, (1 - t_R)$ presented in Eq. 6, are dependent upon the block coefficient C_B . The normal rudder force F_N is defined in terms of the rudder aspect ratio and the effective speed of water flow over rudder (Kijima et al., 1999, Fujii et al., 1961). l_{CB} is the length from center of buoyancy to amidship.

Wind Loads

Wind load formulations in actual sea situation

The wind forces and moments acting on the ship can be expressed in terms of ship steady speed, that is:

$$\begin{aligned} X_A &= C_{AX}(\psi_A) q_A A_F \\ Y_A &= C_H C_{AY}(\psi_A) q_A A_L \\ N_A &= C_H C_{AN}(\psi_A) q_A A_L L_{OA} \\ K_A &= C_H C_{AK}(\psi_A) q_A A_L H_L \\ q_A &= \frac{1}{2} \rho_A U_A^2 \end{aligned} \quad (7)$$

with C_{AX}, C_{AN} etc.; the wind force and moment coefficients, presented in the next section, depended on relative wind direction ψ_A , C_H ; the heel effect coefficient, ρ_A ; the air density, U_A ; the relative wind velocity, L_{OA} ; the overall length, A_F ; the frontal projected area, A_L ; the lateral projected area and H_L ; the mean height of a ship (equal to A_L/L_{OA}).

The relative wind velocity for longitudinal and lateral directions u_x, u_y , based on the coordinated system with the true wind velocity U_T and direction ψ are,

$$\begin{aligned} u_x &= U_T \cos \psi + U \cos \beta \\ u_y &= U_T \sin \psi - U \sin \beta \end{aligned} \quad (8)$$

Then the relative wind velocity U_A and direction ψ_A are calculated using next equations:

$$\begin{aligned} U_A^2 &= u_x^2 + u_y^2 = U_T^2 + U^2 + 2U_T U \cos(\psi + \beta) \\ \psi_A &= \tan^{-1} \frac{u_x}{u_y} = \tan^{-1} \frac{U_T \cos \psi + U \cos \beta}{U_T \sin \psi - U \sin \beta} \end{aligned} \quad (9)$$

The authors (Fujiwara et al., 2006b) used the following definition as the dynamic pressure in the actual sea wind conditions:

$$q_A = q_T + q_S + 2\sqrt{q_T \cdot q_S} \cos(\psi + \beta) \quad (10)$$

where

$$\begin{aligned} q_S &= \frac{1}{2} \rho_A U^2 \\ q_T &= q_{HL} \quad \text{for } X_A \\ q_T &= k_q \cdot q_M + (1 - k_q) q_{HL} \quad \text{for } Y_A, N_A, K_A \\ q_{HL} &= \frac{\rho_A U_T'^2}{2} \Big|_{H_L} \\ q_M &= \frac{1}{H_L} \int_{H_L} \frac{\rho_A U_T'^2(z_A) dz_A}{2} \end{aligned} \quad (11)$$

with the air density ρ_A . The correction method devised by Blendermann (1995) is applied to take care of different wind profiles. The variable q_{HL} , the dynamic pressure at the bridge height H_{BR} , together with q_M , the mean dynamic air pressure measured from water surface up to a location corresponding to the mean height H_L are introduced in Eq. 11. Additionally k_q is an empirical parameter varying with q_M/q_{HL} with a maximum value of 1.0 as indicated in:

$$k_q = 2.162 \left(\frac{q_M}{q_{HL}} \right)^2 - 2.422 \left(\frac{q_M}{q_{HL}} \right) + 1.260 \quad \text{in } 0.50 \leq q_M/q_{HL} \leq 1.00 \quad (12)$$

A ship located in the boundary layer of a realistic wind velocity profile, for example, a one-seventh law, has been assumed to be a windy sea condition. U_T' is the wind velocity at z_A using the standard height z_{AI} where is the above point of 10m from ground and defined as power law in next.

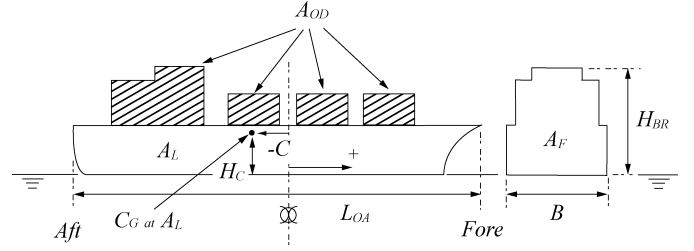


Fig. 2 Definitions of each parameter on ship form in the wind force and moment estimations

$$U_T' = U_T \left(\frac{z_A}{z_{AI}} \right)^{\alpha_A} \quad (13)$$

The power law parameter α_A depended on the actual sea condition is calculated as (Fujiwara et al., 2006b):

$$\alpha_A = 1/(-0.20U_T + 12.0) \quad (14)$$

The heel effect coefficient C_H with ϕ (rad.) is decided as follows using the experimental results of the models with heel angle (Kruppa et al., 1965, Okada, 1952):

$$C_H = 0.355\phi + 1.0 \quad (15)$$

Estimation of wind load coefficients

The authors proposed the new estimation method of wind force coefficients C_{AX}, C_{AY} and moment coefficients C_{AN}, C_{AK} , which has the best accuracy level rather than the previous methods, using the physical components, namely the longitudinal-flow drag, cross-flow drag, lift and induced drag (Fujiwara et al., 2006a). The reference system origin is located at the intersection of the undisturbed free-surface, the amidship section of the ship, where the levers for estimating yaw moment and heel moment are defined with respected to this point of intersection.

To estimate wind force and moment coefficients, the 8 basic hull form parameters, illustrated in Fig. 2, are used in the equations. Here, B ; the breadth, A_{OD} ; the lateral projected area of superstructure etc. on the deck, C ; the horizontal distance from amidships section to center of lateral projected area, H_C ; the height from calm water surface to center of lateral projected area, H_{BR} ; the height of top of superstructure (bridge etc.) in addition to L_{OA} , A_F , A_L .

The longitudinal and lateral wind force coefficients C_{AX}, C_{AY} are defined as follows:

$$\begin{aligned} C_{AX}(\psi_A) &= F'_{LF} + F'_{XLI} + F'_{ALF} \\ &= C_{LF} \cos \psi_A \\ &\quad + C_{XLI} \left(\sin \psi_A - \frac{1}{2} \sin \psi_A \cos^2 \psi_A \right) \cdot \sin \psi_A \cos \psi_A \\ &\quad + C_{ALF} \sin \psi_A \cos^3 \psi_A \end{aligned} \quad (16)$$

Table 1. Coefficients of non-dimensional parameter in the wind load estimating equations

	i	j	0	1	2	3	4
α_j			0.404	0.368	0.902		
β_{ij}	1		-0.922	0.507	1.162		
	2		0.018	-5.091	10.367	-3.011	-0.341
γ_{ij}	1		0.116	3.345			
	2		0.446	2.192			
δ_{ij}	1		0.458	3.245	-2.313		
	2		-1.901	12.727	24.407	-40.310	-5.481
ε_{ij}	1		-0.585	-0.906	3.239		
	2		-0.314	-1.117			

$$C_{AY}(\psi_A) = F'_{CF} + F'_{YLI} \\ = C_{CF} \sin^2 \psi_A \\ + C_{YLI} (\cos \psi_A + \frac{1}{2} \sin^2 \psi_A \cos \psi_A) \cdot \sin \psi_A \cos \psi_A \quad (17)$$

$F'_{LF}, F'_{XLI}, F'_{ALF}$ mean the terms of longitudinal-flow drag, lift and induced drag, and additional longitudinal drag, respectively. And F'_{CF}, F'_{YLI} are the cross-flow drag, and lift and induced drags in the lateral direction components. Each coefficient in Eq. 16 and 17 is obtained from the following equations.

The cross-flow and longitudinal-flow coefficient C_{CF} & C_{LF} ;

$$C_{CF} = \alpha_0 + \alpha_1 \frac{A_F}{BH_{BR}} + \alpha_2 \frac{H_{BR}}{L_{OA}} \quad (18)$$

$$C_{LF}^{0^\circ \leq \psi \leq 90^\circ} = \beta_{10} + \beta_{11} \frac{A_L}{L_{OA} B} + \beta_{12} \frac{C}{L_{OA}} \\ C_{LF}^{90^\circ \leq \psi \leq 180^\circ} = \beta_{20} + \beta_{21} \frac{B}{L_{OA}} + \beta_{22} \frac{H_C}{L_{OA}} + \beta_{23} \frac{A_{OD}}{L_{OA}^2} + \beta_{24} \frac{A_F}{B^2} \quad (19)$$

The lift and induced drag coefficient C_{YLI} in the term of F'_{YLI} ;

$$C_{YLI} = \pi \frac{A_L}{L_{OA}^2} + C_{YM} \quad (20)$$

The first term in the Eq. 20 stands for the liner lift component and the second is the corrective term affected from ship hull form above sea level. The coefficients C_{YM} separated in the wind direction are,

$$C_{YM}^{0^\circ \leq \psi \leq 90^\circ} = \gamma_{10} + \gamma_{11} \frac{A_F}{L_{OA} B} \\ C_{YM}^{90^\circ \leq \psi \leq 180^\circ} = \gamma_{20} + \gamma_{21} \frac{A_{OD}}{L_{OA}^2} \quad (21)$$

The lift and induced drag coefficient C_{XLI} in the term of F'_{XLI} ;

$$C_{XLI}^{0^\circ \leq \psi \leq 90^\circ} = \delta_{10} + \delta_{11} \frac{A_L}{L_{OA} H_{BR}} + \delta_{12} \frac{A_F}{BH_{BR}} \\ C_{XLI}^{90^\circ \leq \psi \leq 180^\circ} = \delta_{20} + \delta_{21} \frac{A_L}{L_{OA} H_{BR}} + \delta_{22} \frac{A_F}{A_L} + \delta_{23} \frac{B}{L_{OA}} + \delta_{24} \frac{A_F}{BH_{BR}} \quad (22)$$

Moreover, the coefficient C_{ALF} in the term of F'_{ALF} is defined as follows:

$$C_{ALF}^{0^\circ \leq \psi \leq 90^\circ} = \varepsilon_{10} + \varepsilon_{11} \frac{A_{OD}}{A_L} + \varepsilon_{12} \frac{B}{L_{OA}} \\ C_{ALF}^{90^\circ \leq \psi \leq 180^\circ} = \varepsilon_{20} + \varepsilon_{21} \frac{A_{OD}}{A_L} \quad (23)$$

The values of each coefficient are shown in Table 1.

The yaw and heel moment coefficients are represented using the lateral wind force C_Y like these:

$$C_N(\psi_A) = C_Y(\psi_A) \cdot L_N(\psi_A) \\ = C_Y(\psi_A) \cdot \left[0.927 \times \frac{C}{L_{OA}} - 0.149 \times (\psi_A - \frac{\pi}{2}) \right] \quad (24)$$

$$C_K(\psi_A) = C_Y(\psi_A) \cdot L_K \\ = C_Y(\psi_A) \cdot (0.0737 \times \left(\frac{H_C}{L_{OA}} \right)^{-0.821}) \quad \text{for } \frac{H_C}{L_{OA}} \leq 0.097 \\ = C_Y(\psi_A) \cdot 0.500 \quad \text{for } \frac{H_C}{L_{OA}} > 0.097 \quad (25)$$

This wind loads estimation method has the same accuracy level as the authors' previous method (Fujiwara et al., 1998), which was more accurate than the earlier reported prediction methods, and has more rational form of estimation rather than the previous one.

Wave Loads

Wave loads are assumed as the sum of the components of resistance increase caused by ship motion, X_{W0} , and wave drift forces X_{WI} etc. due to the diffraction of short waves as follows:

$$X_W = X_{W0} + X_{WI} \\ Y_W = Y_{WI} \\ N_W = N_{WI} \quad (26)$$

X_{W0} is obtained using the proposed method of Fujii et al. (1967) that modifies Maruo(1957)'s method. The ship motion response in regular waves used in the Fujii's method is calculated by NSM (New Strip Method). The terms using the suffice WI mean the wave drift force components caused by the wave reflection on hull surface, which is calculated by the method of one of the authors (Ueno et al., 2000).

The terms of wave loads in the short crested irregular waves are defined as follows:

Table 2. Principal particulars for large passenger ship

Principal particulars		Calm water resistance	
L_{OA} (m)	275.7	R_0	-2.33E-02
L_{PP} (m)	242.2	R_1	3.98E-01
B (m)	36.0	R_2	-3.67E+00
d (m)	8.40	R_3	1.48E+01
W (t)	52001	R_4	-2.18E+01
GM (m)	1.78	Propeller	
KG (m)	17.8	D_p (m)	5.50
l_{CB} (m)	3.55	l_{fp}	0.795
C_B	0.710	l_{wp0}	0.708
C_P	0.730	P (m)	5.49
C_{PA}	0.800	Rudder	
C_{WA}	0.980	A_R (m ²)	32.1
A_T (m ²)	1600.7	Λ	1.43
A_H (m ²)	10189.4	h (m)	6.77
A_{OD} (m ²)	4419.3	l_{tr}	0.749
C (m)	-6.87	a_{H1}	0.533
H_{BR} (m)	40.5	x'_{H1}	-0.975
H_C (m)	19.5	x'_{R}	-0.471
H_r (m)	37.0	z'_{R}	0.560

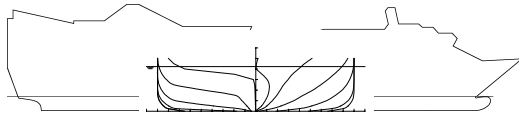


Fig. 3 Side profile and body plan of large passenger ship

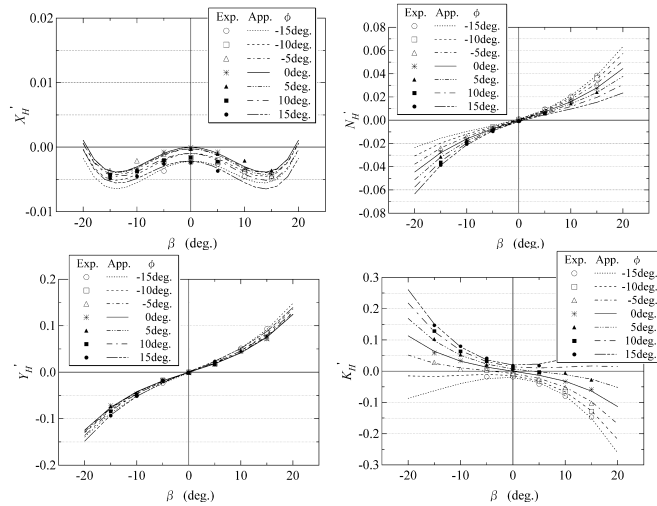


Fig. 4 Experimental hydrodynamic force and moment coefficients and approximated lines of underwater hull for large passenger ship

$$\begin{aligned} X_{W0} &= C'_{WX0} q_W L_{PP} \\ X_{W1} &= C'_{WX1} q_W L_{PP} \\ Y_{W1} &= C'_{WY1} q_W L_{PP} \\ N_{W1} &= C'_{WN1} q_W L_{PP}^2 \end{aligned} \quad (27)$$

where

$$q_W = \frac{1}{2} \rho g \zeta^2. \quad (28)$$

ρ , ζ are the water density and the wave amplitude in irregular waves. The non-dimensional coefficients C'_{WX0} , C'_{WX1} etc., using the wave

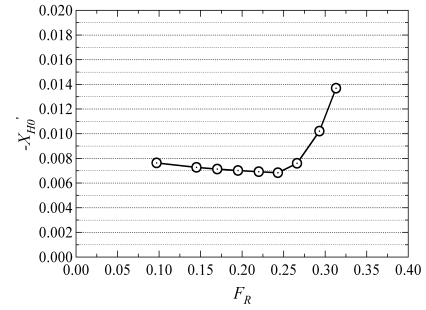


Fig. 5 Resistance coefficient X'_{H0} of large passenger ship in calm water at $\beta, \phi = 0^\circ$

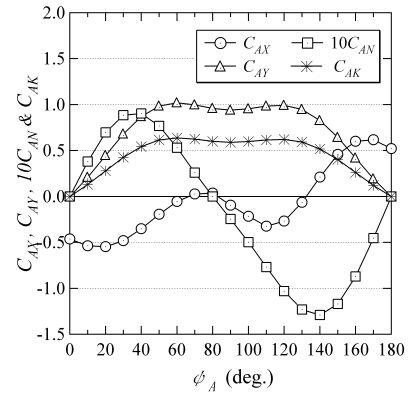


Fig. 6 Wind force and moment coefficients of large passenger ship

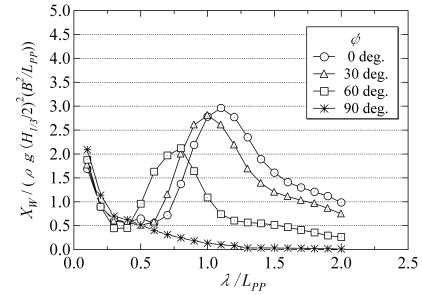


Fig. 7 Longitudinal wave force coefficients of large passenger ship

resistance and wave drift coefficients in regular waves C_{WX0} , C_{WX1} etc, the wave spectrum $S(\omega)$, the wave direction form $G(\mu)$, are shown as follows in case of C'_{WX0} , for example:

$$C'_{WX0} = \frac{1}{m_0} \int_{-\pi/2}^{\pi/2} \int_0^\infty C_{WX0} S(\omega) G(\mu) d\omega d\mu \quad (29)$$

where

$$\begin{aligned} m_0 &= \int_0^\infty S(\omega) d\omega \\ S(\omega) &= \frac{A}{\omega^5} \exp\left(\frac{-B}{\omega^4}\right), \quad A = \frac{173H_{1/3}^2}{T_{01}^4}, \quad B = \frac{691}{T_{01}^4} \end{aligned} \quad (31)$$

$H_{1/3}$, T_{01} are the significant wave height and the wave period. ω is the circular frequency. Empirical form of wave direction $G(\mu)$ with the dominant wave direction μ , which coincides with wind direction, is

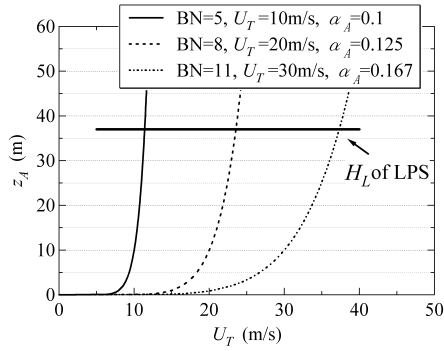


Fig. 8 Wind velocity profiles with Beaufort number BN and power law parameter α_A , compared with the averaged height H_L of large passenger ship (LPS)

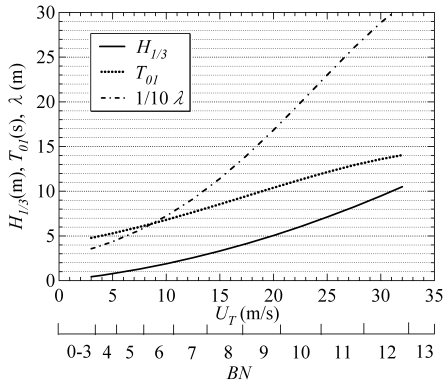


Fig. 9 Weather condition in the sea around Japan for significant wave height $H_{1/3}$, wave period T_{01} and length λ for steady wind velocity U_T with Beaufort number BN

used as:

$$G(\mu) = \frac{2}{\pi} \cos^2 \mu \quad \left(-\frac{\pi}{2} \leq \mu \leq \frac{\pi}{2}\right). \quad (32)$$

CALCULATED CONDITION

A large passenger ship, shown in Fig. 3 for the side profile and the body plan and presented in Table 2 for principal particulars, is treated in this paper. In the Table 2, each coefficient means C_B ; the block coefficient of a ship, C_p and C_{PA} ; the prismatic coefficients of whole hull and aft part of a ship hull, C_{WA} ; the water plane area coefficient of aft hull, w_{p0} ; the propeller wake coefficient, P ; the propeller pitch, A_R ; the rudder area, Λ ; the aspect ratio of the rudder, h ; the rudder height. The ship has two propellers and two rudders, though one-unit specifications are only noted in the table. The ship has no trim.

The hydrodynamic forces and moments used in the calculation for different drift and heel angles are shown in Fig. 4. In the figures, the approximated lines are also drawn with the results of each heel angle. Fig. 5 shows the resistance coefficient X'_{H0} in calm water at $\beta, \phi=0^\circ$. The wind load coefficients were estimated by the method of the previous section (Fujiwara, 2006a) as shown in Fig. 6, and non-dimensional wave loads summed two kinds of wave forces, calculated

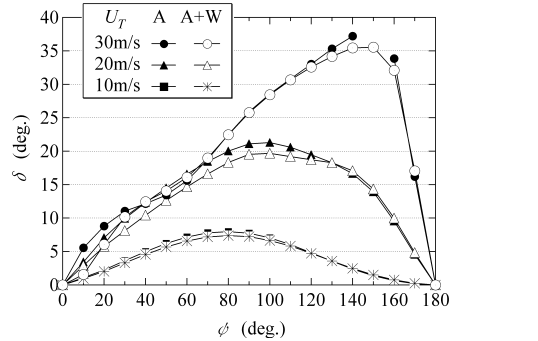
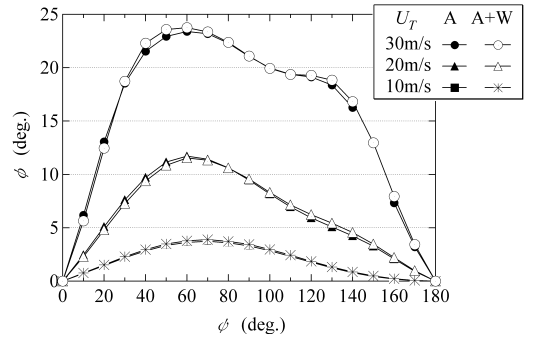
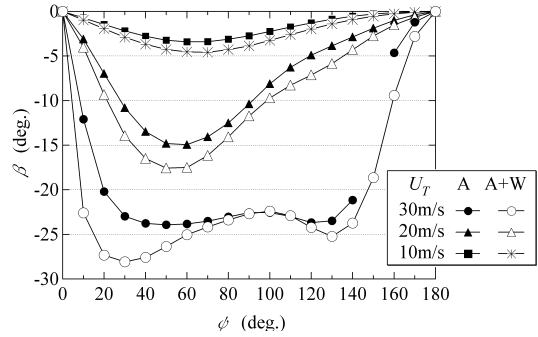
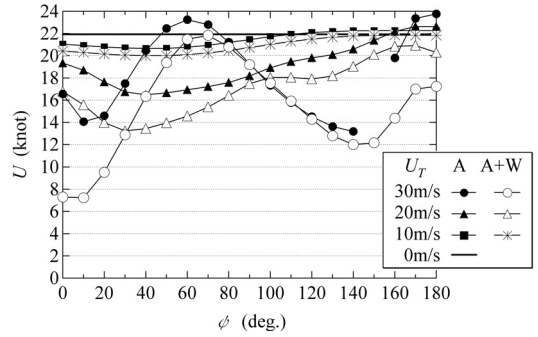


Fig. 10 Calculated results of ship speed loss, drift, heel and rudder angles for large passenger ship in wind and waves

by the method of Fujii et al. (1967) and Ueno(2000), are also presented in Fig. 7. Propeller rotation was set to the constant value, $n=119\text{rpm}$, which the ship can run with 22.0knot in calm water and no wind.

Wind velocity profiles with the power law parameter α_A and Beaufort number (BN), compared with the averaged height H_L of large passenger ship, are shown in Fig. 8. In the strong wind, the difference of the wind setting between the power law profile assumed in actual sea and the constant one used usually in the past is very large. Weather

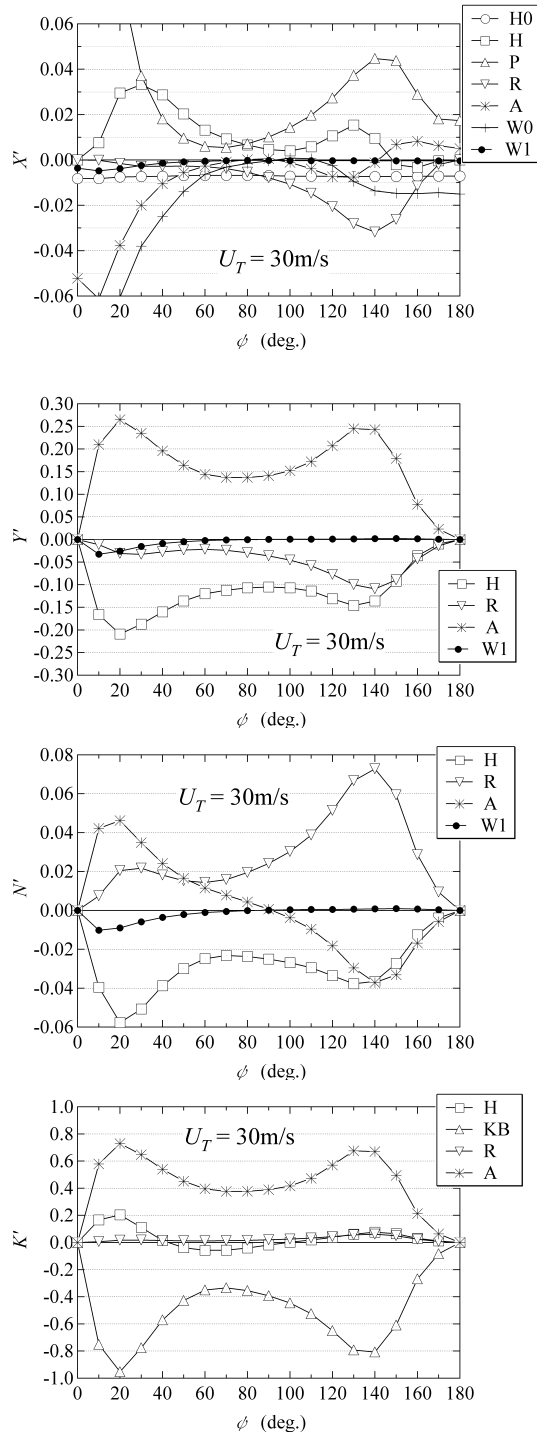


Fig. 11 Separated components of non-dimensional force induced by wind and waves on large passenger ship in $U_T=30\text{m/s}$

condition used in the calculation for significant wave height $H_{1/3}$, wave period T_{01} and length λ for steady wind velocity U_T are also shown in Fig. 9. The wave conditions caused by wind were derived from the weather database in the sea around Japan (Tsujiyama, 2005).

CALCULATED RESULTS

The calculated results for the steady advance speed of the ship, drift, heel and rudder angles, U , β , ϕ & δ are shown in Fig. 10. The wind velocities U_T are set to 10, 20, 30m/s. The black marks with 'A' means the results with only wind external forces, and white marks with 'A+W' means the ones with wind and waves. Fig. 11 shows the separated components of non-dimensional force induced by wind and waves on the large passenger ship in $U_T=30\text{m/s}$. Each results' line means that H0; calm water resistance, H; drift and heel effects on hull resistance, P; propeller thrust, R; rudder, and A; wind forces, W0; wave resistance caused by ship motion, W1; wave drift forces and KB; buoyancy, respectively.

In case of strong wind $U_T=30\text{m/s}$ and about $40\text{deg.} \leq \psi \leq 50\text{deg.}$ in Fig. 10, the drift of the ship becomes more than 25deg. and the heel angle also more than 20deg. The rudder angle has maximum value in back side oblique wind in about $\psi=150\text{deg.}$ The large passenger ship with large superstructures is greatly affected by wind and waves. The assessment of the resistance increase for all wind directions is very important since maximum speed loss dose not only present in the head windy condition.

In all wind direction, the ship speed is reduced by the effect of wind and waves. The assessment of the resistance increase for all wind directions is very important since the speed loss is largely affected by wind direction. In some strong windy case of $50\text{deg.} \leq \psi \leq 70\text{deg.}$ and $160\text{deg.} \leq \psi \leq 180\text{deg.}$, the large passenger ship gets the thrust from wind rather than the other wind directions.

One understands from the results of Fig. 10, comparing with the results of 'A' and 'A+W', that the large passenger ship is greatly affected by wind. The tendency of the results of 'A' is not rapidly changed to the results of 'A+W'.

In case of the condition with only wind, 'A', the large passenger ship cannot keep steady balance in broad reach wind about $\psi=150\text{deg.}$ but in case of 'A+W' the ship can cruise in steady condition since the ship goes straight with slower speed than the condition of 'A' and then the propeller thrust increases relatively.

In case of the strong windy condition, for example $U_T=30\text{m/s}$, the speed loss of the large passenger ship is very large in the wind direction $0\text{deg.} \leq \psi \leq 40\text{deg.}$ and $120\text{deg.} \leq \psi \leq 160\text{deg.}$ The speed loss of the alternative wind direction is mainly caused by the resistance of rudder as shown in Fig. 11. The rudder forces give the great influence on C_X , C_Y , C_N .

Increased DHP (Delivered Horse Power) ratio, R_{DHP} (%) for large passenger ship due to wind and waves is calculated using the following definitions.

$$R_{DHP} = \frac{DHP}{DHP_{nw}} \times 100 \quad (\%) \quad (33)$$

$$DHP = 2\pi K_Q(J) \rho n^3 D_p^5 / 735.5$$

Here, DHP_{nw} ; DHP with no wind and waves (ps), $K_Q(J)$; torque coefficient.

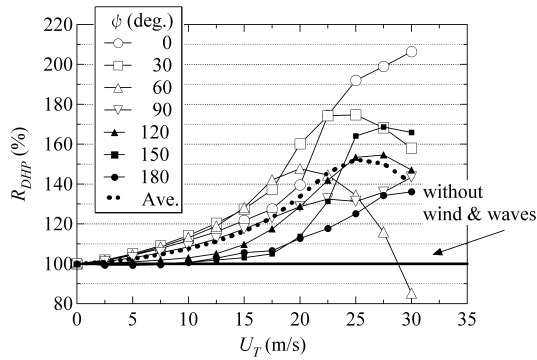


Fig. 12 Increased DHP ratio (R_{DHP}) for large passenger ship due to wind and waves

The results of R_{DHP} are shown in Fig. 12. The horizontal axis is wind velocity U_T . This figure shows the tendency of R_{DHP} is depended on wind direction ψ . In case of $\psi=60\text{deg.}$, as shown in Fig. 10 in windy situation, R_{DHP} value decrease in more than $U_T=20\text{m/s.}$

When the ship speed becomes slower, the torque coefficient $K_Q(J)$ increases since the propeller rotation n has a constant value in the calculation. As a result, in $U_T=30\text{m/s}$ and $\psi=0\text{deg.}$ the R_{DHP} exceeds 200% compared with the condition of no wind and waves. These results are obtained from the one of the calculated assumptions, but it can be understood that it is under the situation that the larger propeller load is provided to the ship engine.

CONCLUSIONS

The authors presented the new estimation method of wind loads acting on ships based on the physical-component-model of the wind loads. The steady cruising performances of the large passenger ship are estimated under strong wind and waves using the new wind loads estimation method. The results of this paper are summarized as follows:

1. Cruising performances of a large passenger ship in heavy wind and waves are clearly understood using the latest wind loads estimation method that has the best accuracy level rather than the previous methods. In the calculation, the effect of wind profiles is adopted to estimate the exact performances of the ship in heavy sea.
2. In all wind direction, the ship speed is reduced by the effect of wind and waves. The assessment of the resistance increase for all wind directions is very important since the speed loss is largely affected by wind direction.
3. Comparing with the results with only wind and wind & waves external forces, the large passenger ship with large superstructures is influenced from wind rather than waves. The speed loss of the wind direction $120\text{deg.} \leq \psi \leq 160\text{deg.}$ is mainly caused by the resistance of rudder.
4. In case of only wind forces, the large passenger ship with constant propeller rotation cannot keep steady balance in back side oblique wind about $\psi=150\text{deg.}$
5. Increased DHP ratio for a large passenger ship due to wind and waves is calculated and presented in various kinds of wind velocities and directions.

REFERENCES

- Blendermann W (1995). "Estimation of wind loads on ships in wind with a strong gradient," *Proc 14th International Conference on Offshore Mechanics and Arctic Engineering (OMAE1995)*, Vol.1-A, 1995, pp271-277.
- Fujii H and Takahashi T (1967). "On the Increase in the Resistance of a Ship in Regular Head Sea (in Japanese)," *Mitsubishi Heavy Industries Technical Review*, Vol.4 No.6, pp86-92.
- Fujii H and Tsuda T (1961). "Experimental Researches on Rudder Performance (2) (in Japanese)," *J Society of Naval Architects of Japan*, Vol.110, pp31-.
- Fujiwara T, Hearn G.E, Kitamura F, Ueno M, and Minami Y (2005). "Steady Sailing Performance of a Hybrid-sail assisted Bulk Carrier," *Int J Marine Science and Technology*, Vol.10 No.3, The Society of Naval Architects of Japan, pp131-146.
- Fujiwara T, Ueno M and Ikeda Y (2006a). "A New Estimation Method of Wind Forces and Moments acting on Ships on the basis of Physical Component Models (in Japanese)," *J The Japan Society of Naval Architects and Ocean Engineers*, Vol.2, pp243-255.
- Fujiwara T, Ueno M and Ikeda Y (2006b). "Cruising performance of ships with large superstructures in heavy sea – 1st report: Added resistance induced by wind – (in Japanese)," *J The Japan Society of Naval Architects and Ocean Engineers*, Vol.2, pp257-269.
- Fujiwara T, Ueno M and Nimura T (1998). "Estimation of Wind Forces and Moments acting on Ships (in Japanese)," *J the Society of Naval Architects of Japan*, Vol.183, pp77-90.
- Hirano M, Takashina J (1982). "A Calculation of Ship turning Motion taking coupling Effect due to Heel into Consideration," *J the West-Japan Society of Naval Architects*, Vol.59, pp71-81.
- Kansai Shipbuilding Design Handbook (1983). The Kansai Society of Naval Architects, Japan, p465.
- Kijima K, Katsuno T, Nakiri Y et al. (1990). "On the Manoeuvring Performance of a Ship with the Parameter of Loading Condition," *J Society of Naval Architects of Japan*, Vol.168, pp141-148.
- Kijima K, Nakiri Y (1999). "Approximate Expression for Hydrodynamic Derivatives of Ship Manoeuvring Motion taking into account of the Effect of Stern Shape (in Japanese)," *J the West-Japan Society of Naval Architects*, Vol.98, pp67-77.
- Kruppa and Henschke W et al. (1965). "Seitliche Luft- und Wasserkräfte bei Schräganströmung von Fahrgastschiffen und Fischereifahrzeugen," *Schiffbauforschung* 4, pp97-125.
- Maruo H (1957). "On the Increase of the Resistance of a Ship in Rough Seas (in Japanese)," *J Society of Naval Architects of Japan*, Vol.108, pp5-13.
- Naito S, Takagishi K (1998). "Time Mean Behavior of Large Full Ships in the Sea (in Japanese)," *J The Kansai Society of Naval Architects, Japan*, pp57-68.
- Okada S (1952). "On the Heeling Moment due to the Wind Pressure on Small Vessels (in Japanese)," *J Society of Naval Architects of Japan*, Vol.92, pp75-81.
- Ueno M, Nimura T, Miyazaki H and Nonaka K (2000). "Steady Wave Forces and Moment acting on Ships in Manoeuvring Motion in Short Waves (in Japanese)," *J Society of Naval Architects of Japan*, Vol.188, pp163-172.
- Yuasa M, Suzuki K, Tataka Y (1986). "On Hull Response of ships in Service (1st Report: Hull Response of a Pure Car Carrier) (in Japanese)," *J Society of Naval Architects of Japan*, Vol.159, pp217-228.
- Tsujimoto M and Ishida S (2005). "Statistical Characteristics of Winds and Waves around Japan," *Proc Fifteenth ISOPE*, pp108-115.